American Mineralogist, Volume 72, pages 312–318, 1987

Solid-solution thermodynamics in $CaCO_3$-$MnCO_3$

CHRISTOPHER CAPOBIANCO,* ALEXANDRA NAVROTSKY*
Departments of Chemistry and Geology, Arizona State University, Tempe, Arizona 85287, U.S.A.

ABSTRACT

Thermodynamic mixing data are reported for the calcite-rhodochrosite solid-solution series. Enthalpies of solution in an aqueous solvent saturated in NaCl and containing 0.745 *M* HCl were obtained for $CaCO_3$-$MnCO_3$ samples prepared at 600°C. The enthalpy of mixing is, in kcal/mol,

$$\Delta H^{mx} = (X)(1 - X)[1.493 \pm 0.099 + (13.17 \pm 0.29)X - (73.19 \pm 0.91)X^2 + (60.27 \pm 0.63)X^3],$$

where X is the mole fraction of $MnCO_3$. Isothermal phase-equilibrium relations between CO_2, MnO, and $(Mn_XCa_{1-X})CO_3$ at 700°C gave the excess free energy of mixing across the join as

$$\Delta G^{ex}_{700°C}/RT = (X)(1 - X)[1.120 \pm 0.068 + (0.538 \pm 0.012)X].$$

Positive excess free energies and complex enthalpies (both endo- and exothermic deviations) imply negative excess entropies of mixing. Asymmetric enthalpy behavior is also inferred from phase-equilibrium data. This behavior is seen in materials without the long-range Mn-Ca ordering characteristic of kutnahorite.

INTRODUCTION

The join $CaCO_3$-$MnCO_3$ is a bounding binary in the rock-forming carbonate tetrahedron, but carbonate solid solutions with other than minor or trace amounts of Mn are relatively rare. However, Mn-bearing calcites are found in and around ore bodies, especially epithermal Pb-Zn and Ag deposits (Tsusue, 1967). Additionally, many of the natural occurrences have been described from regionally metamorphosed manganiferous terranes (e.g., Zak and Povandra, 1981; Wenk and Maurizo, 1978). In these latter instances, Mn-bearing calcites are often associated with other minerals in which Mn is a major component, commonly in solid solution with Ca components (Peters et al., 1978; Winter et al., 1981). Geochemical interpretations of manganiferous assemblages and certain ore deposits will be facilitated given knowledge of the thermodynamics of mixing for Ca and Mn. This study provides data pertinent to Ca-Mn mixing in rhombohedral carbonate phases.

Beneath the ocean floor, Mn-bearing calcites have been found as precipitates on foraminifera tests (Boyle, 1983). Authigenic Mn-bearing calcites in subsurface deep-sea sediments from the Panama Basin have also recently been discovered (Penderson and Price, 1982). The latter authors have reported several other submarine occurrences and have noted that the kutnahorite composition is commonly found. Kutnahorite is the compound having the dolomite structure in the calcite-rhodochrosite system. The prevalence of the kutnahorite composition in submarine environments is somewhat surprising. At temperatures of the ocean floor, the development of dolomite-type order within Mn-bearing calcites is kinetically unlikely, and actual ordered phases are undocumented. Understanding of these low-temperature occurrences is hindered by a sparse thermodynamic data base for solid solutions in this system.

Previous data on the thermodynamics of mixing in this system can be obtained only from phase-equilibria studies (e.g., Goldsmith and Graf, 1957; Boynton, 1971; de Capitani and Peters, 1981). This study reports solution calorimetric data for a series of six supersolvus synthetic solid solutions across the calcite-rhodochrosite binary join. New high-temperature phase-equilibria experiments are also presented to further constrain the thermodynamics of mixing.

EXPERIMENTAL METHODS

Phase-equilibrium experiments involving $(Ca,Mn)CO_3$ decomposition

The purpose of these experiments was to obtain the activity coefficient of $MnCO_3$ in the carbonate solid solution at 700°C as a function of composition. This was done by finding the satu-

* Present addresses: (Capobianco) Department of Earth Sciences, University of Cambridge, Cambridge, England. (Navrotsky) Department of Geological and Geophysical Sciences, Princeton University, Princeton, New Jersey 08544, U.S.A.

0003–004X/87/0304–0312$02.00

TABLE 1. Data from 700°C (Ca, Mn)CO_3 decomposition runs

Run	Duration (h)	P_{CO_2} (psi)	a_m* (Å)	α** (°)	2θ†
3	138	7250	6.2660(7)	46.395(7)	40.58
10	288	11800	6.0335(13)	47.182(14)	40.57
13	146	12420	5.9752(62)	47.375(59)	40.56
14	96	10900	6.1166(36)	46.905(38)	40.56
16	102	1520	6.3597(6)	46.106(6)	40.56
17	98	8960	6.2220(9)	46.538(9)	40.55
19	147	9080	6.2234(14)	46.534(14)	40.54
22	173	9700	6.2000(15)	46.657(17)	40.56
28	122	10550	6.1295(19)	46.857(27)	40.56

* Rhombohedral unit-cell length.
** Rhombohedral cell angle.
† Two-theta angle for (200) peak in MnO, Cu$K\alpha$.

TABLE 2. Unit-cell parameters and compositions from microprobe analysis for (Ca, Mn)CO_3 phases

a_m	α	X_{MnCO_3}
6.3756(9)	46.077(10)	0.0000(2)
6.3238(9)	46.219(9)	0.1184(70)
6.2771(5)	46.359(4)	0.2023(60)
6.1628(23)	46.745(3)	0.4308(120)
6.1060(6)	46.939(6)	0.5550(160)
5.9446(6)	47.545(6)	0.9154(20)
5.9010(9)	47.764(10)	1.000(2)

ration concentration of $MnCO_3$ in the solid solution coexisting with a pure MnO phase and a CO_2 fluid of known fugacity.

Experiments were conducted in a cold-seal hydrothermal apparatus using CO_2 as a pressure medium. Run pressure was monitored using a Bourdon-tube gauge with 20-psi graduations up to 30000 psi. The run temperature was monitored from the external thermocouple well on a standard 1.25 in. (3.18 cm) cold-seal vessel using a chromel-alumel thermocouple which was periodically calibrated against the melting point of KBr at 686°C. Two experimental charges were included in each equilibration. Each charge of 3–5 mg of starting material (consisting of an undersaturated carbonate plus MnO and an oversaturated carbonate plus MnO) was wrapped in silver foil and held at run conditions for durations between 96 and 228 h. The MnO phase was obtained by decarbonation of previously recrystallized $MnCO_3$. The carbonate solid solutions used for starting material were obtained by techniques discussed below. The location of the saturation surface in compositional space was approached from either side, and therefore these runs were considered reversed when the X-ray films from each run produced experimentally indistinguishable patterns.

The oxygen fugacity of the CO_2 fluid was not buffered except by the pressure vessel itself. All successful runs contained only MnO as the oxide phase, which sets an upper limit on $\log(f_{O_2})$ at 700°C of -14. Under these conditions, the CO/CO_2 ratio is so low that the CO_2 pressure can be accurately approximated by the total pressure. Huebner (1969) found the decomposition temperature of pure $MnCO_3$ to be insensitive to f_{O_2} variation. No attempt to control f_{O_2} was justified for this study.

The equilibrium run conditions are reported in Table 1. The pressure for a given run is accurate to ± 50 psi. The temperature was maintained constant at 700($\pm$2)°C. The composition obtained from X-ray data assuming Vegard's law is reported at the level of precision of the lattice-parameter refinements (i.e., ± 0.001 mol fraction). The error bars on the coefficients of the derived activity-coefficient equation were obtained using a Monte Carlo method of propagation of errors from the uncertainties given above (see Anderson, 1976).

Synthesis and characterization of samples for solution calorimetry

Samples along the calcite-rhodochrosite join were initially precipitated from concentrated aqueous solutions of the chlorides by adding excess K_2CO_3. The precipitate was rinsed, dried, and subsequently recrystallized under CO_2 pressure (8000–15000 psi) at 600°C in crimped Pt capsules. Not all samples resulting from this procedure produced crystals large enough for analysis by microprobe. Microprobe analyses for samples with large enough grain size are reported in Table 2 (based on at least 10 analyses from separate grains) along with the refined lattice parameters of samples used to construct a working curve. The lattice parameters for all carbonate materials in this study were obtained from refined X-ray powder patterns using an internal standard of Si with Guinier camera techniques. Several previous workers have reported an essentially linear relation between composition and unit-cell length (Goldsmith and Graf, 1957; de Capitani and Peters, 1981; Fubin and Stone, 1983). Our data confirm these results and justify the Vegard's law assumption for compositional estimates.

Calorimetric techniques

After preliminary experiments with several aqueous and molten salt solvents at 80–350°C, an aqueous solvent saturated in NaCl and containing 0.745 M HCl at room temperature was adopted. The high-ionic-strength acid brine has a low vapor pressure and a low CO_2 solubility and rapidly dissolves carbonates reproducibly at 85°C. Heats of solution were obtained in this solvent using a Tian-Calvet heat-flow calorimeter operating at 85°C. An advantage of this solvent is the small magnitude of the heats of solution. To permit unequivocal interpretation of the enthalpies of mixing obtained from the enthalpies of solution in this chemically complex solvent, several precautions were taken. (1) The heat of mixing at a given composition along the $CaCO_3$-$MnCO_3$ join was found by comparing the measured heat of solution of the solid solution with the measured heat of solution of a mechanical mixture of endmember carbonates at the same composition as the solid solution. (2) The volume of solvent and the mass of all samples dissolved were held strictly constant for all runs (20.0-mg samples were dissolved in 20 mL of solvent). This procedure made it unnecessary to correct for the work done in CO_2 evolution or to unravel the complex chemical interactions within the solvent. The thermochemical cycle used with this technique is therefore very simple. For a given composition X,

$$(Ca_{1-X}Mn_X)CO_{3(xl)} \rightarrow \text{dissolved aqueous components} + CO_{2(gas)}$$
$$(1-X)CaCO_{3(xl)} + (X)MnCO_{3(xl)} \rightarrow \text{dissolved aqueous components} + CO_{2(gas)}$$

Since the right sides of both reactions are the same, even with regard to the number of moles of reactants and products and the concentrations of dissolved components, the difference between the heats of solution gives the enthalpy of mixing at X.

Prior to dissolution, samples were encapsulated in thin-walled pyrex tubes to prevent prereaction of the samples with the corrosive solvent. After thermal equilibrium was attained in the

TABLE 3. Activity for (Ca, Mn)CO_3 solutions at 700°C and 902.6 bars

Run	X_{MnCO_3}	ln γ_{MnCO_3}
16	0.035	1.1682
3	0.233	0.8425
17	0.327	0.7207
19	0.324	0.7436
22	0.374	0.6683
14	0.551	0.4022
28	0.523	0.4204
10	0.727	0.2082
13	0.851	0.1045

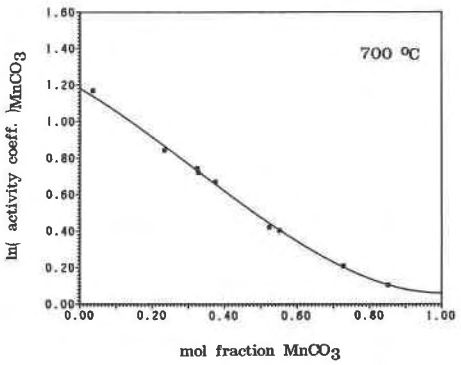

Fig. 1. Activity coefficient vs. composition for $MnCO_3$ component at 700°C. A least-squares curve is shown, and experimental points are from decomposition phase equilibrium.

calorimeter, runs were initiated by crushing the pyrex sample tube. The dissolution was completed within 30 s, but the resulting calorimetric peak lasted between 1 and 2 h because of the long time constant of the large-volume calorimeter used. The total heat effect measured was about 1 cal. Further details of the experimental method are found in Capobianco (1986).

EXPERIMENTAL RESULTS AND THERMODYNAMIC ANALYSIS

Carbonate decomposition experiments

The experimental data reported in Table 1 pertain to the equilibrium three-phase assemblage in the following chemical equilibrium:

$$MnCO_3(xl) = MnO(xl) + CO_2(fluid). \quad (1)$$

X-ray data given in Table 1 indicate that the MnO phase remains essentially unchanged for these isothermal runs regardless of the pressure of equilibration. Because of this, information pertaining to the activity coefficient of $MnCO_3$ is readily available from these P,T,X_{MnCO_3} points. The standard state for Reaction 1 is defined as 700°C and the pressure at which pure $MnCO_3$ is in equilibrium with its pure oxide constituents. This pressure is 902.6 bars as calculated from data given in Robie et al. (1984) for $MnCO_3$ and CO_2 fugacities of Holloway (1977) as 902.6 bars.

The activity of the $MnCO_3$ component in the carbonate is derived from these polybaric, isothermal experiments by simplifying the following general expression:

$$\mu^{P_0}_{MnCO_3} + \int_{P_0}^{P_1} V_{MnCO_3}\, dP + RT_0 \ln a^{P_0}_{MnCO_3} + RT_0 \int_{P_0}^{P_1} \frac{d(\ln a_{MnCO_3})}{dP}\, dP = \mu^{P_0}_{MnO} + \int_{P_0}^{P_1} V_{MnO}\, dP + \mu^{P_0}_{CO_2} + \int_{P_0}^{P_1} \frac{d(\mu_{CO_2})}{dP}\, dP. \quad (2)$$

The PV integrals range from the standard state (P_0,T_0) to the experimental equilibration conditions (P_1,T_0). Since the oxide and fluid are pure and there is no excess volume in the carbonate solid solution, Equation 2 is simplified to the following equation, in which differences in compressibilities and thermal expansivities of the solid phases have been neglected:

$$RT_0 \ln a_{MnCO_3} = RT_0 \ln(f^{P_1}_{CO_2}/f^{P_0}_{CO_2}) + (V_{MnO} - V_{MnCO_3})(P_1 - P_0). \quad (3)$$

Equation 3 was used to calculate values of ln γ_{MnCO_3} activity coefficients reported in Table 3. Positive deviations from ideality are indicated across the entire join as seen in Figure 1. The least-squares regression curve for these data is also plotted and was obtained by consideration of the function $g(X)$, defined as

$$g(X) = \ln \gamma_{MnCO_3}/(1 - X_{MnCO_3})^2. \quad (4)$$

If $g(X)$ does not vary with composition, the solid solution is a regular solution. However, our data indicate more complicated mixing behavior for the calcite-rhodochrosite system. The mathematical form chosen to represent $g(X)$ in the least-squares regression is a polynomial with an appended hyperbolic term:

$$g(X) = \sum_{n=0}^{m} A_n(1 - X_{MnCO_3})^n + \frac{A}{(1 - X_{MnCO_3})^2}. \quad (5)$$

The A parameter, with no subscript, allows the fitted activity coefficient curve to be displaced along the ordinate axis (see Fig. 1) and results from errors in standard thermodynamic data, in CO_2 fugacities, and in measured P and T values. If one does not include this term and attempts, instead, to use a higher-degree polynomial to represent the data, experimentally unwarranted curvature is introduced into the activity-composition relationship. The equation represented in Figure 1 is given by

$$\ln \gamma_{MnCO_3} = (0.0597 \pm 0.0411) + (2.1968 \pm 0.0640)(1 - X_{MnCO_3})^2 - (1.0773 \pm 0.0241)(1 - X_{MnCO_3})^3. \quad (6)$$

The constant (A) on the right-hand side of Equation 5 corresponds to a free-energy discrepancy of 115 cal/mol between the calculated standard state and the 700°C ex-

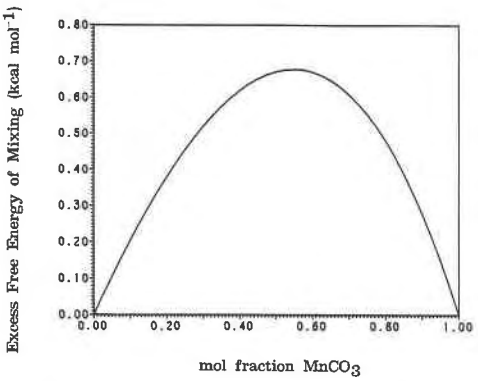

Fig. 2. Excess free energy as a function of composition at 700°C for the calcite-rhodochrosite binary.

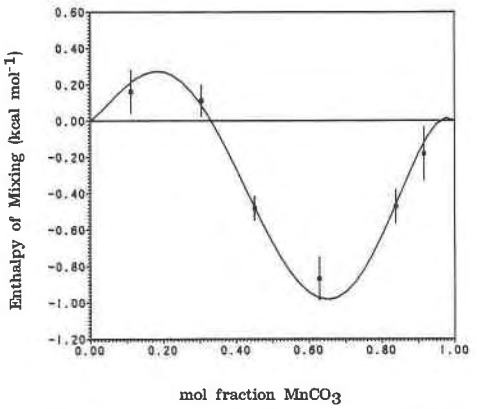

Fig. 3. Calorimetric enthalpy of mixing for 600°C samples and least-squares fit to the data.

periments. This value is within the errors associated with the calculation of the equilibrium standard-state pressure. The mixing relationship is contained only within the last two terms of Equation 6. The leading term is an adjustment to the standard state and is not used below in expressions for the activity coefficient or excess free energy. The errors quoted are standard deviations of the means for the coefficients obtained by regressing Equation 5 fifty times using experimental data (P,T,X) points that have been randomized within their known uncertainties. However, the Monte Carlo statistics are not used for the values of A,A_0,A_1, which are based on the regression of the nominal P,T,X data.

One can apply the Gibbs-Duhem relation to Equation 6 to compute the activity of the $CaCO_3$ component. Equation 7 gives the result.

$$\ln \gamma_{CaCO_3} = (0.5809 \pm 0.0735)(X_{MnCO_3})^2 + (1.0773 \pm 0.0241)(X_{MnCO_3})^3. \quad (7)$$

These last two equations may be combined to give the excess free energy of mixing at 700°C using Equation 8

$$\Delta G^{ex}/RT = X_1 \ln \gamma_1(X) + X_2 \ln \gamma_2(X). \quad (8)$$

One obtains for the calcite-rhodochrosite system

$$\Delta G^{ex}_{700°C}/RT = (X)(1 - X)[1.120 \pm 0.068 + (0.538 \pm 0.012)X], \quad (9)$$

where X is the mole fraction of $MnCO_3$. A plot of ΔG^{ex} at 700°C is shown in Figure 2. The values are everywhere positive with a maximum of 670 cal/mol on the Mn-rich side of the binary. A solvus is anticipated at lower temperatures, but for the 700°C experiments, the convexity of the total free energy of mixing implies a continuous solid solution consistent with known phase behavior.

Calorimetric experiments

The enthalpy of solution data for samples prepared at 600°C are shown in Table 4. The enthalpies of solution of mechanical mixtures do not vary linearly with composition, a fact suggesting complex chemical interaction within the solvent. However, this complexity is of no consequence to the enthalpies of mixing obtained as the difference between enthalpies of solution for mechanical mixtures and solid solutions. The enthalpy of mixing in $CaCO_3$-$MnCO_3$ is shown in Figure 3. Note the highly asymmetric behavior with both positive and negative deviations from ideality.

The least-squares curve represented in Figure 3 was obtained by regression of a function $\lambda(X)$, defined as

$$\lambda(X) = \Delta H^{mx}/(1 - X)(X). \quad (10)$$

This transformation is advantageous because the resulting curve may be fit without constraining it to pass through any nonexperimental points (i.e., at $X = 0$ or $X = 1$ $\Delta H^{mx} = 0$, but $\lambda(X) \neq 0$). This enthalpy-interaction parameter is plotted in Figure 4. Experimental values for the endpoints on this plot have been approximated from the activity-coefficient data derived from the phase-equilibrium experiments. The excess free energies at 600°C for

TABLE 4. Calorimetric data for (Ca, Mn)CO_3 solutions (kcal/mol)

X_{MnCO_3}	0.1124	0.3057	0.4508	0.6278	0.8376	0.9154
			Enthalpies of solution			
ss	2.281(94)	2.877(78)	3.657(42)	4.666(61)	5.142(26)	5.650(77)
mm	2.442(70)	2.987(31)	3.175(49)	3.798(99)	4.670(87)	5.469(121)
			Enthalpies of mixing			
	0.161(117)	0.111(84)	−0.482(65)	−0.868(117)	−0.472(90)	−0.182(144)

Note: ss = solid solutions; mm = mechanical mixtures; values in parentheses represent standard deviation in last decimal place.

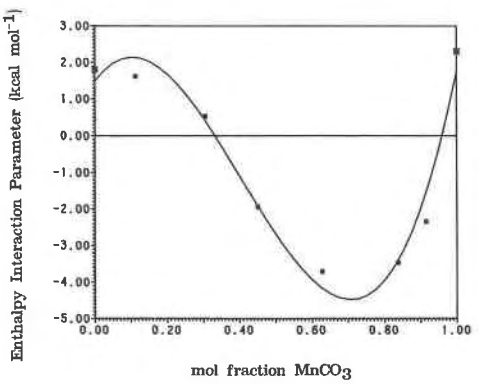

Fig. 4. Enthalpy interaction parameter vs. composition for calcite-rhodochrosite binary. Asterisks are extrapolated from phase-equilibrium data; squares are calorimetric data.

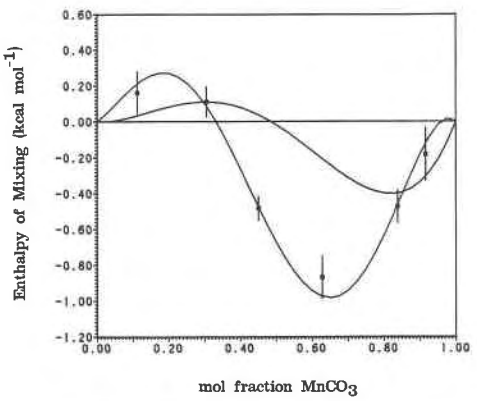

Fig. 5. Enthalpy of mixing from 600°C samples with least-squares curve and enthalpy of mixing obtained from the temperature dependence of excess-free-energy functions. Note the similar shape of the functions.

$MnCO_3$ in $CaCO_3$ at infinite dilution and for $CaCO_3$ in $MnCO_3$ at infinite dilution ($RT \ln \gamma$) are 1941 and 2875 cal/mol, respectively. These values correspond to $\lambda(X)$ at $X = 0$ and $X = 1$, respectively, if at these extreme compositions there is no excess entropy. The other assumption in this approximation is that we may use the 700°C data to represent enthalpies at 600°C; this is not unreasonable if the first assumption is true. The auxiliary data, constraining the endpoints, do not produce any curvature inconsistent with the calorimetric data plotted in Figure 4. However, the positive value for the $MnCO_3$ endpoint causes very slight endothermic behavior for ΔH^{ex} very near pure $MnCO_3$. The least-squares curve shown in Figure 4 is a cubic polynomial (in mole fraction $MnCO_3$) and results in the enthalpy of mixing given by

$$\Delta H^{mx} = (X)(1 - X)[1.493 \pm 0.099 + (13.17 \pm 0.29)X - (73.19 \pm 0.91)X^2 + (60.27 \pm 0.63)X^3]. \quad (11)$$

As in the activity-coefficient fit, the errors in Equation 11 are estimated by standard deviations of the means of regression coefficients from separate data sets generated through Monte Carlo error propagation.

Discussion

The asymmetry of the enthalpy of mixing is extreme for the 600°C samples. Isothermal addition of $CaCO_3$ to pure $MnCO_3$ causes a rapid stabilization of the energy of the phase, whereas adding $MnCO_3$ to pure $CaCO_3$ results in an endothermic maximum. The composition corresponding to the Ca-rich maximum is not well constrained, but falls near $X_{MnCO_3} = \frac{1}{6}$. Perhaps the phase can begin to stabilize in energy only when Mn is in sufficient concentration that the average Ca-O octahedron is linked to at least one Mn.

The central region of the binary indicates modest energy stabilization. Since the phase-equilibrium data show positive excess free energies, the exothermic heats of mixing imply significant excess entropies of mixing. It is tempting to relate the observed negative excess enthalpy and inferred negative excess entropy to the influence of (Ca,Mn) ordering analogous to that in the ordered low-temperature phase, kutnahorite. However, greater symmetry with respect to the 50:50 composition might be expected if these results were wholly attributable to kutnahorite formation. Also, the temperature of formation of the solid solution (600°C) is well above that at which kutnahorite disorders, and the X-ray patterns of the synthetic materials show no dolomite-type reflections. It is possible that the asymmetry is due to the superposition of more than one energetically distinct intracrystalline process.

A partial separation of the energetic contributions to the calorimetric enthalpy of mixing can be done using the phase-equilibrium work of Boynton (1971). He determined an isothermal (90°C) excess-free-energy curve for the calcite-rhodochrosite system from aqueous solution/crystal partition coefficients for Ca and Mn. He forced the solid phases in his solution-precipitation experiments to maintain homogeneous composition, even at this low temperature, by an external cycling of CO_2 pressure. The excess free energy (expressed as a function of X_{MnCO_3}) derived from his experiments is represented by

$$\Delta G^{ex}/RT = (X)(1 - X)(1.0745 + 2.6288X - 4.1101X^2). \quad (12)$$

However, Equation 12 does not produce a stabilization at or near the kutnahorite composition as expected if his data referred to a stable equilibrium involving the ordered phase. Boynton did demonstrate that his data represented equilibrium values, but it is probable that the equilibrium was metastable involving only disordered carbonate solid solutions. This is useful for the present discussion because it permits a calculation of the temperature differential of the excess free energy of mixing in a continuous carbonate solid solution without the influence of kutnahorite.

The excess free energy of our study showed no evidence for kutnahorite because it was obtained from samples well above the stability field of kutnahorite (700°C).

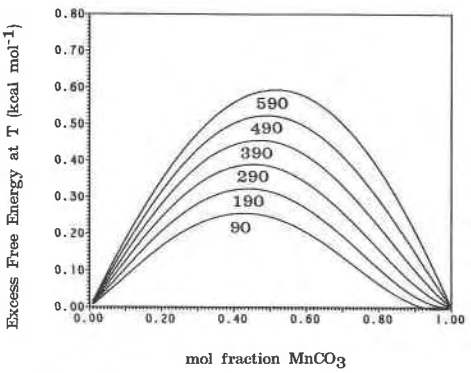

Fig. 6. Excess-free-energy curves at 100-deg intervals from 90 to 590°C. Note that the excess free energy increases with temperature. Calculations refer to phases with no Ca-Mn ordering.

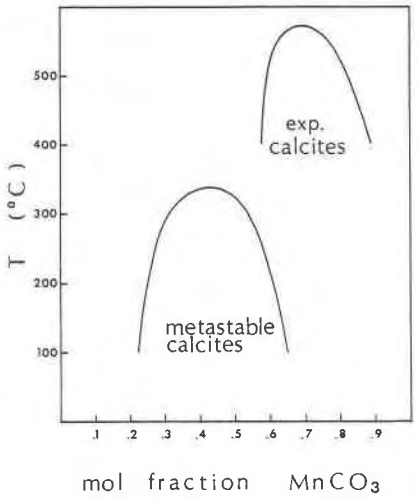

Fig. 7. Phase diagram for calcite-rhodochrosite. Experimental solvus given by de Capitani and Peters (1981); metastable solvus calculated from temperature-dependent excess-free-energy functions given in this study.

Boynton's data (90°C) did not exhibit stabilization near kutnahorite presumably because kinetic factors inhibited the ordering process. Since both data sets are isothermal determinations, one can calculate a simple temperature differential for ΔG^{ex}:

$$(\Delta G^{ex}_{700°C}/RT - \Delta G^{ex}_{90°C}/RT)/(700 - 90) \simeq d(\Delta G^{ex}/RT)/dT. \quad (13)$$

The derivative is assumed independent of temperature and is given by

$$d(\Delta G^{ex}/RT)/dT \simeq 10^{-3}(0.0739 - 3.427X + 6.738X^2). \quad (14)$$

This approximation to the temperature dependence of the excess free energy of mixing in the (assumed to be) completely disordered solid solution can be compared to the calorimetric data by using the Gibbs-Helmholtz equation:

$$d(\Delta G^{ex}/RT)/dT = -\Delta H^{ex}/RT^2. \quad (15)$$

One can use this equation to calculate a metastable excess enthalpy at 600°C. This function along with the calorimetrically determined excess enthalpy for samples prepared at 600°C are plotted in Figure 5. Notice that the derived excess enthalpy curve exhibits similar asymmetric behavior to the calorimetric data. Apparently the asymmetry is unrelated to the kutnahorite ordering process.The calorimetric function shows larger exothermic effects in the central region. The difference between these functions is perhaps the enthalpic effect of partial ordering at 600°C. Alternatively, the additional energy stabilization may have been acquired during quench.

The above observations are consistent with the following ideas about the kutnahorite order-disorder process. At 700°C (the temperature of phase-equilibrium studies), no significant long- or short-range order exists. Samples quenched from 600°C contain some short-range order, either present at T or produced during quench. They are not long-range ordered. If the short-range order persists at 600°C, then, since the onset of disordering for an initially long-range ordered kutnahorite is 450°C (Goldsmith and Graf, 1957), one must conclude that disordering occurs over a rather large temperature interval. Analogous relations among long-range and short-range order and their energetic effects have been discussed for Mg_2TiO_4 (Wechsler and Navrotsky, 1984).

To distinguish the above possibilities, calorimetric samples quenched from other temperatures will be required.The variation of the calorimetric excess enthalpy with annealing could then be used to assess possible reordering effects [see Reeder and Wenk (1983) for the case of $CaMg(CO_3)_2$] and to estimate the total enthalpy required to disorder kutnahorite. In either case, kutnahorite is stable by at least 0.63 kcal/mol in enthalpy relative to a disordered solid solution, as indicated by the difference in enthalpy of mixing derived from the calorimetric and from the phase-equilibrium data.

A METASTABLE SOLVUS IN $MnCO_3$-$CaCO_3$

The effect of the suppression of kutnahorite ordering on the phase behavior is seen in a calculation of a metastable solvus using Equation 14. The derived temperature dependence of the excess free energy of mixing may be used to calculate a mixing curve at all temperatures between 90 and 700°C. A plot of the excess free energy for 100-deg intervals is shown in Figure 6. The calculated excess free energies increase with increasing temperature. Negative excess entropies are again inferred, but now for mixing processes that exclude ordering due to kutnahorite. The calculated solvus is shown in Figure 7 along with the experimentally determined solvus of de Capitani and Peters (1981). The metastable solvus closes at 355°C, whereas the experimental solvus extends to about 550°C. Solid solubility is generally increased in this system when kutnahorite-forming processes are suppressed. Carbonate

phases with compositions near kutnahorite, or even beneath the stable solvus, may therefore sometimes be representative of metastable interphase equilibrium. It has been suggested (Tsusue, 1967, among others) that a Ca-rich solvus should exist in this system at temperatures too low for solid-state phase-equilibrium experiments. The present data are insufficient to calculate the presumed phase behavior (analogous to the Ca-Mg system) since we lack necessary thermodynamic information on kutnahorite. However, the metastable solvus offers an alternative explanation for natural metamorphic samples that do not exhibit immiscibility on the Mn-rich side of the join (see Essene, 1983). One should also be aware that naturally coexisting Ca-rich and kutnahorite-composition phases do not necessarily confirm the analogy with the Ca-Mg system, unless the 50:50 phase can be shown to contain kutnahorite ordering.

Conclusion

We have found, by two independent methods (calorimetry and phase-equilibrium studies), that the enthalpy of mixing within the calcite-rhodochrosite binary is very asymmetric. The more volatile carbonate component ($MnCO_3$) causes a slight energy destabilization of calcite, and the refractory component ($CaCO_3$) produces initial exothermic mixing effects in rhodochrosite. The crystal-chemical interpretation of this behavior awaits further structural characterization. We have inferred the presence of significant negative excess entropies from both the calorimetric and phase-equilibria data. An additional exothermic enthalpy effect observed in the calorimetric data has been attributed to short-range kutnahorite order that either persists considerably above the onset of disordering for kutnahorite or is acquired during quench. Finally, we suggest that some naturally occurring phases of kutnahorite composition might be better termed "pseudokutnahorite" since they may be formed without any dolomite-type ordering.

Acknowledgments

This work was supported by the National Science Foundation, Solid State Chemistry Program, Grants DMR 8106026 and DMR 8521562.

References

Anderson, G.M. (1976) Error propagation by the Monte Carlo method in geochemical calculations. Geochimica et Cosmochimica Acta, 40, 1533–1538.

Boyle, E.A. (1983) Manganese carbonate overgrowths on foraminiferal tests. Geochimica et Cosmochimica Acta, 47, 1815–1819.

Boynton, W.V. (1971) An investigation of the thermodynamics of calcite-rhodochrosite solid solutions. Ph.D. Thesis, Carnegie-Mellon University, Pittsburgh.

Capobianco, C. (1986) Thermodynamic relations among several carbonate solid solutions. Ph.D. Thesis, Arizona State University, Tempe, Arizona.

de Capitani, C., and Peters, T. (1981) The solvus in the system $MnCO_3$-$CaCO_3$. Contributions to Mineralogy and Petrology, 76, 394–400.

Essene, E.J. (1983) Solid solutions and solvi among metamorphic carbonates with applications to geologic thermobarometry. Mineralogical Society of America Reviews in Mineralogy, 11, 77–96.

Fubin, B., and Stone, F.S. (1983) Physico-chemical properties of $MnCO_3$-$CaCO_3$ and MnO-CaO solid solutions. Journal of the Chemical Society, Faraday Transactions 1, 79, 1215–1227.

Goldsmith, J.R., Graf, D.L. (1957) The system CaO-MnO-CO_2: Solid solution and decomposition relations. Geochimica et Cosmochimica Acta, 11, 310–334.

Holloway, J.R. (1977) Fugacity and activity of molecular species in supercritical fluids. In D.G. Fraser, Ed. Thermodynamics in geology, p. 161–181. D. Reidel, Boston.

Huebner, J.S. (1969) Stability relations of rhodochrosite in the system manganese-carbon-oxygen. American Mineralogist, 54, 457–481.

Pendersen, T.F., and Price, N.B. (1982) The geochemistry of manganese carbonate in Panama basin sediments. Geochimica et Cosmochimica Acta, 46, 59–68.

Peters, T., Trommsdorff, V., and Sommerauer, J. (1978) Manganese pyroxenoids and carbonates: Critical phase relations in metamorphic assemblages from the Alps. Contributions to Mineralogy and Petrology, 66, 383–388.

Reeder, R.J., and Wenk, H.R. (1983) Structure refinements of some thermally disordered dolomites. American Mineralogist, 68, 769–776.

Robie, R.A., Haselton, H.T., and Hemingway, B.S. (1984) Heat capacities and entropies of rhodochrosite ($MnCO_3$) and siderite ($FeCO_3$) between 5 and 600 K. American Mineralogist, 69, 349–357.

Tsusue, A. (1967) Magnesian kutnahorite from Ryujiima mine, Japan. American Mineralogist, 52, 1751–1763.

Wechsler, B., and Navrotsky, A. (1984) Thermodynamics and structural chemistry of compounds in the system MgO-TiO_2. Journal of Solid State Chemistry, 55, 165–180.

Wenk, H.R., and Maurizio, R. (1978) Kutnahorite, a rare Mn mineral from Piz Cam (Bergell Alps). Schweizerische Mineralogische und Petrographische Mitteilungen, 58, 97–100.

Winter, G.A., Essene, E.J., and Peacor, D.R. (1981) Carbonate and pyroxenoids from the manganese deposit near Bald Knob, North Carolina. American Mineralogist, 66, 278–298.

Zak, L., and Ponvondra, P. (1981) Kutnahorite from the Chvaletice pyrite and manganese deposit, east Bohemia. Tschermaks Mineralogische und Petrographische Mitteilungen, 28, 55–63.

Manuscript received May 22, 1986
Manuscript accepted November 20, 1986